AIAA-2000-2392

Review of Skin Friction Measurements Including Recent High-Reynolds Number Results from NASA Langley NTF

R. D. Watson, R. M. Hall, and J. B. Anders
NASA, Langley Research Center
Hampton, VA 23681

Fluids 2000
19-22 June 2000 / Denver, CO

AIAA PAPER 2000-2392

REVIEW OF SKIN FRICTION MEASUREMENTS INCLUDING RECENT HIGH-REYNOLDS NUMBER RESULTS FROM NASA LANGLEY NTF

Ralph D. Watson*
Flow Physics and Control Branch

Robert M. Hall†
Configuration Aerodynamics Branch

John B. Anders*
Flow Physics and Control Branch

NASA, Langley Research Center
Hampton, Virginia 23681

ABSTRACT

This paper reviews flat plate skin friction data from early correlations of drag on plates in water to measurements in the cryogenic environment of The NASA Langley National Transonic Facility (NTF) in late 1996. The flat plate (zero pressure gradient with negligible surface curvature) incompressible skin friction at high Reynolds numbers is emphasized in this paper, due to its importance in assessing the accuracy of measurements, and as being important to the aerodynamics of large scale vehicles. A correlation of zero pressure gradient skin friction data minimizing extraneous effects between tests is often used as the first step in the calculation of skin friction in complex flows. Early data compiled by Schoenherr for a range of momentum thickness Reynolds numbers, R_θ, from 860 to 370,000 contained large scatter, but has proved surprisingly accurate in its correlated form. Subsequent measurements in wind tunnels under more carefully controlled conditions have provided inputs to this database, usually to a maximum R_θ of about 40,000. Data on a large axisymmetric model in the NASA Langley National Transonic Facility extends the upper limit in incompressible R_θ to 619,800 using the van Driest transformation. Previous data, test techniques, and error sources are discussed, and the NTF data will be discussed in detail. The NTF Preston tube and Clauser inferred data accuracy is estimated to be within – 2 percent of a power-law curve fit, and falls above the Spalding theory by 1 percent at R_θ of about 600,000.

1. INTRODUCTION

The design of transport aircraft requires that accurate estimates of skin friction be made at length Reynolds numbers around 10^9 and Mach numbers of approximately 0.8, corresponding to cruise conditions[1]. This estimate is often made by first calculating the flat plate incompressible skin friction and then correcting for various effects such as pressure gradient, three-dimensionality of the flow, compressibility, etc. Several baseline theories/correlations are available, most of which differ in the skin friction level predicted at high Reynolds numbers where there has been a dearth of data.

As will be shown, the most commonly used correlations of skin friction do not agree to the

* Senior Member AIAA
† Associate Fellow AIAA

desired accuracy at high Reynolds numbers, and it is not clear which method is the most accurate. Over the years, compilations and critical reviews of the available data have been made, but only recently has skin friction data at very high Reynolds numbers become available. The most recent data is usually tunnel wall data, with the exception of the present data which was taken on a large axisymmetric model.

An experiment to measure flat plate skin friction at flight Reynolds numbers was conducted in the Langley National Transonic Facility, NTF. The purpose of the test was to provide skin friction data at very high Reynolds numbers to compare with existing theories. The difficulties in measuring skin friction free of extraneous effects and to the desired accuracy was recognized early. In addition to the usual problems associated with testing at high Reynolds numbers, the cryogenic environment of the tunnel affected both the model and instrumentation and complicated the test. A description of the test, the results obtained, and comparison with other available skin friction data will be discussed.

A factor to be considered in testing at high unit Reynolds numbers is the difference in scales between the wall and the outer region. At the wall, the turbulent scales are so small that wall roughness may be an important factor —*i.e.*, the wall must be very carefully machined to avoid roughness-induced effects. What for most engineering purposes would be considered adequate wall smoothness may not be the case at high Reynolds numbers[2]. Another of the many problems is the difficulty of manufacturing boundary layer rakes with tubes spaced closely enough to capture the law-of-the-wall region.

2. NOMENCLATURE

c_f	friction coefficient
c_p	pressure coefficient
C	constant in equation 7
d	outside diameter of Preston tube
D	model diameter, 12.75 inches
E	constant in equation 2
H	shape factor, δ^*/θ
k	van Driest constant, equation 7
M	Mach number
r	radial coordinate
R	unit Reynolds number, $\rho u/\mu$
s	distance along surface of model
T	temperature
u	velocity, fps
u_τ	shear velocity, $(\tau_w/\rho)^{1/2}$
u^+	u/u_τ
x	axial distance along model
y	coordinate normal to surface
y^+	$y\, u_\tau/\upsilon$
α	angle of attack of model
β	Clauser pressure gradient parameter, $(\delta^*/\tau)\,(dp/dx)$
δ	boundary layer thickness
δ_u	thickness at $u/u_e = 0.99$
δ^*	displacement thickness
δ^+	value of y^+ at edge of boundary layer
θ	momentum thickness, inches
μ	dynamic viscosity
υ	kinematic viscosity
ρ	density
τ	shear stress
ϕ	roll angle on model, see Figure 4

subscripts

aw	adiabatic wall condition
e	at edge of boundary layer
i	incompressible
t	stagnation condition
w	at wall
x	based on x coordinate
θ	based on θ
∞	freestream condition

superscript

reduced to incompressible form by Van Driest method (equation 6) for velocities and integral quantities, or by Sommer and Short T method (equation 5) for temperature-dependent quantities

3. NTF EXPERIMENT

The NTF test was designed to accurately measure adiabatic flat plate skin friction values at Reynolds numbers as high as possible and Mach numbers corresponding to flight conditions in order to extend the existing skin friction-Reynolds number database. The highest Reynolds numbers obtainable in Langley Research Center tunnels are produced in the cryogenic transonic tunnels,

NTF and 0.3 M Transonic Tunnel. For this test, unit Reynolds numbers as high as 94 x 10^6/ft were run, and length Reynolds numbers of 940 x 10^6 at the downstream measurement station on the model were measured. The difficult task of measuring skin friction in the cryogenic tunnels is made even more difficult by model and instrumentation problems related to the extreme low temperature of the flow.

The idea of a test for obtaining high Reynolds number c_f data in NTF is not new, and in fact, a program to do so was outlined by Saric[3]. The ideas presented in this report were used in planning the NTF test, the major difference being the model on which c_f was to be measured. It was determined in the early planning stage that a two-dimensional flat plate posed too many problems in mounting and maintaining the accuracy of the surface in the high dynamic pressure environment. For this reason an axisymmetric model was designed for which transverse curvature effects were small, based on the thickness of the predicted boundary layer. In addition, it was necessary to account for compressibility effects at Mach numbers as high as 0.8 in order to transform the data to an equivalent incompressible state.

It was decided that no new skin friction measuring techniques would be developed for this test, since development was considered too time-consuming for an experiment in NTF. It was also required to measure the skin friction as accurately as possible, a notoriously difficult measurement to make, even at ambient temperature. Three different standard techniques were used with the rationale that they would either provide consistency among themselves or point out inadequacies in the experiment. A skin friction balance was used since it is the only way to measure skin friction directly. Also used were Preston tubes and boundary layer surveys, from which skin friction was inferred by a modified Clauser method. There has been a renewed interest in the validity of the law of the wall lately, as evidenced in the report of George and Castillo[4]. The law of the wall is used extensively here to present data and to infer c_f from velocity profile measurements. The surveys were also necessary to determine the boundary layer integral quantities such as the momentum and displacement thicknesses.

A photograph of the model in NTF is shown in Figure 1.

4. FLAT PLATE SKIN FRICTION DATA AND THEORY

4.1 Theories and Correlations

Schoenherr s correlation of his own data and the data of others dating to 1872[5] was published almost 70 years ago, but is still used in its correlated form, except at low Reynolds numbers. Skin friction was obtained from the drag of plates of various sizes towed in water and, not surprisingly, the data exhibits large scatter when plotted as a function of Reynolds number. When correlated with an equation of von Karman, the results agree with most carefully-controlled experiments. Twenty years later, in 1953, the paper by Landweber was published[6], describing the characteristics of turbulent boundary layers and deriving a shear law that agreed closely with the method of Schoenherr. Nine years after this, the method of Spalding[7] was published. This method was derived from his sublayer-buffer-log profile, but did not account for the outer portion of the boundary layer. If the usual law of the wall constants are used in Spalding s c_f equation the answer is incorrect, since the wake is not accounted for correctly. The constants were adjusted for use as the incompressible theory in the Spalding-Chi compressible skin friction method[8] to produce a more reasonable c_f level. By adjusting the constants of course, the level can be changed, but, more important, the slope of c_f vs R_θ does not match that of the Karman-Schoenherr correlation over the complete Reynolds number range. Other methods which have been used are Ludwieg-Tillmann[9], and recently, Fernholz and Finley[10], which is based on both inner and outer similarity and is compared with data to R_θ of 200-300 x 10^5.

The Karman-Schoenherr equations are:

$$0.242 / \sqrt{c_F} = \log_{10}\left(c_F R_x\right) = \log_{10}\left(2R_\theta\right)$$
$$c_f = 0.558 c_F / \left(0.558 + 2\sqrt{c_F}\right) \qquad (1)$$

where c_F is the average skin friction coefficient.

The local skin friction coefficient, c_f, was obtained by differentiating the first of the two equations.

The Spalding equations are

$$R_x = \frac{\left(u_e^+\right)^4}{12} + \left(\frac{1}{k^3 E}\right)\left\{e^{ku_e^+}\left[6 - 4ku_e^+ + \left(ku_e^+\right)^2\right] - 6 - 2ku_e^+ - \frac{\left(ku_e^+\right)^4}{12} - \frac{\left(ku_e^+\right)^5}{20} - \frac{\left(ku_e^+\right)^6}{60} - \frac{\left(ku_e^+\right)^7}{252}\right\}$$

$$R_\theta = \frac{\left(u_e^+\right)^2}{6} + \left(\frac{1}{kE}\right)\left[e^{ku_e^+}\left(1 - \frac{2}{ku_e^+}\right) + \frac{2}{ku_e^+} + 1 - \frac{\left(ku_e^+\right)^2}{6} - \frac{\left(ku_e^+\right)^3}{12} - \frac{\left(ku_e^+\right)^4}{40} - \frac{\left(ku_e^+\right)^5}{180}\right] \quad (2)$$

where $c_f = \dfrac{2}{\left(u_e^+\right)^2}$

The Ludwieg-Tillmann equation is

$$c_f = 0.246 \times 10^{-0.678H} \times R_\theta^{-0.268} \quad (3)$$

The Fernholz and Finley equations are

$$\frac{c_f}{2} = \left\{\frac{1}{k}\ln\left(\frac{\Delta u_\tau}{\nu}\right) + C - N + \left(\frac{1}{k} - M\right)\ln\left(\frac{y}{\Delta}\right)_p\right\}^{-2}$$

$$\text{where } \ln\left(\frac{\Delta u_\tau}{\nu}\right) = \ln\left(R_x\right) \cong 0.3 + \ln\left(R_\theta\right) \quad (4)$$

$$\Delta = \int_0^\gamma \frac{(u_e - u)}{u_\tau}\, dy$$

$$\text{and } \ln\left(\frac{y}{\Delta}\right)_p \cong -2.7 \quad \text{for } R_\theta > 2000$$

$$\cong -0.404\, \ln\left(R_\theta\right) + 0.37 \quad \text{for } 4252 < R_\theta < 2000$$

$$k = 0.4,\ C = 5.1,\ M = 4.70,\ \text{and } N = 6.74$$

The methods of Karman-Schoenherr, Spalding, Ludwieg-Tillmann, and Fernholz and Finley are shown in Figure 2. From the figure, it is obvious that the theories do not agree with each other over the complete range of Reynolds numbers. The methods of Karman-Schoenherr and Spalding show opposite trends at low and high Reynolds numbers, the crossover point occurring at R_θ between 6000 and 7000. The Karman-Schoenherr correlation includes Kempf s data to R_θ of about 370,000 (R_x of 450 x 10^6.) The Spalding method relies on the constants of the law-of-the-wall, and thus might be in question at high Reynolds numbers unless these constants are shown to be the same as for lower Reynolds

numbers. Ludwieg-Tillmann deviates from Karman Schoenherr below R_θ about 3000 and above R_θ about 20000. Fernholz and Finley is lower than the other theories.

4.2 Data

Over the past 30 years excellent reviews of available incompressible and compressible boundary layer data have been compiled. These include the compilation for incompressible flows by Coles and Hirst from the Stanford Conference in 1968[11], the compilations of compressible flow data by Fernholz and Finley in 1977[12], and 1981[13], and the examination of Incompressible data to 1996 by Fernholz and Finley[10]. Since that time, other data has been published, most high Reynolds number data having been taken on the wall of wind tunnels. These data appear to be different from flat plate boundary layer data[14], *i.e.*, the boundary layer has developed in regions of wall curvature and strong adverse and favorable pressure gradients, and is usually not characteristic of equilibrium flat plate boundary layers until a sufficiently long run has been made. Relaxation has apparently not been completed before entering the test section.

Reference 15 from 1996, listed data in addition to that of reference 10, but did not present skin friction measurements at high Reynolds numbers. In 1984, Gaudet[16], published data at Mach 0.8 on the sidewall of the RAE 8 ft by 8 ft wind tunnel and reexamined the data of reference 17. Other data was published in 1994 by Motallebi[18] on the wall of a wind tunnel for R_θ from 26,000 to 106,000 in compressible flow; however, skin friction was not measured in all cases and the data are not used for comparison here. The tabulated data of Fernholz, Krause, Nockemann, and Schober[19] is compared in Figure 3 with high Reynolds number data of Gaudet, low Reynolds number data of Coles[20] and Purtell[21], and the methods of Karman-Schoenherr (K-S) and Spalding. For this figure the compressible profiles of Gaudet, were re-reduced and transformed by the van Driest transformation[22], which was also used for the NTF data transformation. Noted in the figure is the R_θ range of the data taken in NTF on an axisymmetric model, and reported in a following section.

The methods of Karman-Schoenherr and Spalding will be used to compare with the present data, since they agree reasonably well with the best experimental data available at this time over a large range of R_θ.

5. NTF EXPERIMENT - RESULTS AND DISCUSSION

5.1 Tunnel, Model, Instrumentation, and Test Conditions

5.1.1 Tunnel The range of operating conditions for the National Transonic Facility (NTF) at Langley Research Center[23] is as follows: Mach numbers from 0.2 to 1.2, total pressure from one to 9 atmospheres, total temperature from —320 to 150deg. F, and Re/ft from 3.7 to 146 x 10^6 at Mach 1. For cryogenic operation, liquid nitrogen is injected into the flow downstream of the test section, and vaporized to maintain low tunnel temperatures. Intermediate temperatures can be attained by regulating the amount of liquid nitrogen injected. The tunnel can also be run using air if no cooling is required. For the present tests, both ambient temperatures and cryogenic temperatures were used to obtain the desired Reynolds number range.

The test section is 25 feet long, and 8.2 ft square[24], making it possible to mount very long models in the tunnel to produce large length Reynolds numbers. The model described here was 17.28 feet long. The test section is slotted to minimize blockage effects, which were 3.3% based on an inviscid geometric area ratio. Measured model pressures demonstrated that the flow over the model was uniform, validating that the slotted design worked as expected.

Standard tunnel data reduction and tunnel instrumentation[25] were used; however, local values of flow parameters on the model were recalculated from measured model conditions using the Fortran routines of NTF. The Beattie-Bridgemann equation of state was used to calculate the properties of both nitrogen and air[26].

5.1.2 Model The design of the model was a compromise among several factors. It was desirable to have a long model in order to produce large length Reynolds numbers. The diameter was required to be large enough so that the model would not deflect significantly under its own weight and to allow room for the balance and other instrumentation to be mounted internally. In addition, it needed to be large enough that transverse curvature effects would not significantly affect skin friction. It could not be too large, or model loads and blockage effects would be excessive.

A sketch of the axisymmetric 347 stainless steel model is shown in Figure 4. It was an

axisymmetric cylinder 12.75 inches in diameter having a nose described by a superellipse, and 7 cylindrical sections downstream of the nose. Ports were installed in the model at Stations 1 and 2, at x=73.95 and 121.95 inches, respectively. Skin friction was measured by a balance and by Preston tubes at Station 2, and by rakes at Stations 1 and 2. The whole model, including the nose, was polished to a surface finish of 4 μ in. No transition trips were used on the nose. The model was sting-mounted in order to minimize boundary layer interference effects, which would be caused by model struts. The NTF sting mount had roll and angle of attack capability that could be used to set the model at nominally zero angle of attack. Initially, Preston tubes were mounted circumferentially around the model to measure the nonuniformity of the flow and adjust the angle of attack.

The design of the nose and flow over the model were predicted using CFD methods. It was determined from these calculations and boundary layer calculations[27] that the pressure gradient would not be a factor in measuring flat plate skin friction. Similarly, the ratio of the boundary layer to the model radius was estimated[27] to be 0.25 at the second measurement station, and transverse curvature effects on c_f were estimated to be less than 1.5 %, at R_θ of about 600,000.

5.1.3 Instrumentation Three methods of determining skin friction on the model were used: a skin friction balance, Preston tubes, and velocity profiles from which skin friction was inferred by the Clauser method. Photographs of the three instruments used on the model are shown in Figure 5. Preston tubes and the skin friction balance were tested at Station 2 at both hot and cold flow conditions. The boundary layer rake was used at Station 1 at the hot flow condition and at Station 2 at hot and cold flow conditions.

The problems associated with the direct measurement of skin friction by balance are well known[28]. Additional problems resulting from operating a mechanical device in a cryogenic environment required that a risk reduction experiment be done in a smaller tunnel — the Langley 0.3 Meter Transonic Cryogenic Tunnel. The problems encountered in the risk reduction experiment were larger than anticipated and greatly influenced the design of the final balance.

Preston tubes were sized from boundary layer calculations. They were designed so that the tube was in the logarithmic region of the boundary layer at all test conditions. It has been shown[29] that the tube can extend well into the wake portion of the boundary layer with no adverse effects; however, the tubes were 0.058 inches in diameter, and did not extend into the outer portion. The nose was unchamfered and polished, and the ratio of internal to external diameter was 0.6. Care was taken in mounting the probes so that the tubes would be firmly attached to the surface and to ensure that no mounting apparatus would protrude into the flowfield (see Figure 5 b).

The only set of Preston tube data know to the authors covering the range of Reynolds numbers for which measurements were to be made was that from Laval University[30]. Rather than rely on a single set of data, a high Reynolds number calibration was made at Princeton University in the Superpipe Facility[2]. The data from the Princeton test was cast in the parameters of four different calibration methods[31-34] to see if any one method gave superior results in determining skin friction from known inputs. It was found that all methods gave the same results. Patel s high Reynolds number calibration was found to predict the Princeton data at high Reynolds numbers, and was used to reduce the NTF data.

Inference of skin friction from velocity surveys is most accurate if tubes on the boundary layer rake are positioned within the logarithmic portion of the turbulent boundary layer. In addition, the edge of the boundary layer should be defined so that the integral quantities δ and δ^* are accurately calculated from the profiles. The boundary layer calculations discussed previously provided the guidelines for tube placement. The tips of the pitot tubes were not chamfered, and were polished, as was done for the Preston tubes

Model pressures were measured by an electronically scanned system, and model temperatures by copper-constantan (Type T) thermocouples accurate to 1 degree K. One port on each ESP module was dedicated to measuring a known reference pressure that was also measured by a secondary standard. Whenever the reference pressure difference deviated by – 0.19% of full scale the modules were re-zeroed online.

5.1.4 Test Conditions The model was tested at Mach numbers from 0.2 to 0.85 and unit Reynolds numbers from 6 x 10^6 to 94 x 10^6 per foot. A matrix of the test conditions is shown in Figure 6. The highest unit Reynolds number was attained at Mach 0.6. The highest unit Reynolds number at

which data could be obtained at Mach 0.85 was 65 x 10^6, a consequence of the load constraints for the model. Noted in the figure are the conditions at which data was obtained on Preston tubes, the balance, and the boundary layer rake. At most tunnel conditions, all three devices were tested, but at Mach 0.7 only Preston tubes were run.

Due to the finite blockage of the model in the tunnel, it was necessary to calculate the local Mach number, which could be slightly different from the freestream Mach number. This was done by averaging pressures at three orifices just ahead of Station 1 and using this pressure as the local static pressure to calculate the nominal local Mach number. To define the model pressure in the vicinity of the measurement stations, 11 orifices around Station 1 and 11 around Station 2 were averaged. These averaged pressures were used as the local static pressure in calculating c_p at their respective stations. Similarily, three temperatures near the two primary data positions were averaged in calculating Tw1 and Tw2.

Representative pressures and temperatures over the model are shown in Figure 7. It is evident that the pressure gradient is sufficiently close to zero and that its effect on the local shear stress can be considered negligible. This is more accurately quantified in later discussion. It is also evident that there is little change in the pressure gradient with Mach number. While not as uniform as the pressure distribution, the model temperature variation is small, being more uniform at ambient temperature, as would be expected.

5.2 Factors affecting NTF Skin Friction Measurements

There are at least seven factors associated with the conditions of the NTF test that can have an effect on measured surface shear. These factors are compressibility, pressure gradient, heat transfer, surface curvature, surface roughness, lateral divergence (three-dimensionality) of the flow, and the freestream disturbance level and scale. All effects, except the freestream disturbance level, were examined before the NTF test was begun to insure that they could be controlled/minimized to the extent that a flat plate skin friction could be measured.

5.2.1 Compressibility Effects Tests were conducted at Mach numbers from 0.2 to 0.85. Above approximately Mach 0.3, compressibility effects must be considered in the flow. One approach, and the one used by Allen in Preston tube reductions[29,31], is the use of the T method. In this method temperature-dependent quantities such as ρ and μ are replaced in parameters and equations by their values at a temperature intermediate between the wall and freestream values -- the T-prime condition. Allen used the Sommer and Short method, which is the Rubesin and Johnson equation with constants determined for Mach 3.82 in air[35]. The Sommer and Short T-prime method was used in this report for all Preston tube reductions. The equation defining the T condition is

$$\frac{T'}{T_e} = 1. + 0.035\, M_e^2 + 0.45\left(\frac{T_w}{T_e} - 1.\right) \qquad (5)$$

In order to present velocity profiles and integral quantities in an equivalent incompressible form, velocity profiles were transformed using the Van Driest method[21], which was shown to transform velocity profiles in the outer region of adiabatic wall boundary layers at Mach 11 in helium[36]. Velocities are transformed in proportion to the density variation from the wall to the edge of the boundary layer by this method; *i.e.*, the vertical coordinate, y, is not transformed.

Called generalized velocities by Maise and McDonald[37], the van Driest transformation is defined as

$$u' = \int_0^u \sqrt{\frac{\rho}{\rho_w}}\, du \qquad (6)$$

With the transformed velocity profile and the density evaluated at the wall, new values of θ, δ^* and u_e result. These transformed properties are used to calculate R_θ and c_f. The transformation was coupled with the Clauser method to infer the shear stress from velocity profiles by an interactive graphical method. The incompressible profile was plotted along with the incompressible law of the wall, and the data was fit to the law of the wall by iteration. It is estimated that the data could be fit to the law of the wall with a resolution of about 0.5 % in c_f by this method. The accuracy of the results are a function of the constants in the law of the wall, defined as

$$\frac{u}{u_\tau} = \frac{1}{k} \ln\left(\frac{y u_\tau}{\upsilon_w}\right) + C \qquad (7)$$

where k=0.41 and C=5.5

The profile data were originally reduced with C=5.0, however it was found that C=5.5 gave a better fit to the Preston tube data and skin friction theory.

5.2.2 Pressure Gradient-Relaxation Effects Preliminary tests were run in the Langley 0.3 Meter Transonic Cryogenic Tunnel, where the effects of both favorable and adverse pressure gradients on measured skin friction were examined. This was accomplished by moving the upper wall of the test section to produce pressure gradients of different magnitude. Figure 8 (a) shows the effects on Preston tube measured c_f in terms of β, the pressure gradient parameter used by Clauser to generate self-similar equilibrium profiles[38]. Data are shown at Mach numbers of 0.6 and 0.8 at two different unit Reynolds numbers, and β_i is a transformed value obtained by using the van Driest transformed value of δ^*. Compressibility and Reynolds number effects are not completely removed using β_i however, the correlation should be adequate for estimating local pressure gradient effects. For these test conditions

$$\frac{c_f}{(c_f)_{\beta_i=0}} = 1. - 0.7\,\beta_i \qquad (8)$$

As shown in Figure 7(a), the pressure gradient on the nose is strongly favorable switching to strongly adverse about x=13 inches, and relaxing to very small adverse pressure gradient about x=30 inches. The pressure gradient is zero at x=50 inches. The question arises as to whether the outer part of the boundary layer had relaxed to the equilibrium zero pressure gradient state by the first measurement station. Station 1 was located at x=73.95 inches, 44 inches from the beginning of small adverse gradient. Measured values of δ and θ were 1.3-1.5 and .065-.075 inches here, or 31 δ and 630 θ from the beginning of small adverse pressure gradient and 17 δ and 340 θ from zero pressure gradient. The distance required for relaxation for flows with adverse pressure gradient followed by zero pressure gradient is about 5-10 δ[39].

5.2.3 Heat Transfer Effects The effect of nonadiabatic wall temperature effects on skin friction were also measured in the 0.3 Meter Tunnel. The total temperature of this tunnel can be rapidly varied from above ambient temperature down to 100 K, making it possible to measure c_f over a range of T_w/T_{aw}. The results are shown in Figure 8 (b) for Mach 0.6 and Mach 0.8. Repeatability is shown by the agreement between two different runs. For most runs in this tunnel, the wall was slightly nonadiabatic due to heat transfer through the tunnel wall to a plenum chamber behind the wall, and then to outside the tunnel.

5.2.4 Transverse Curvature Effects The transverse curvature effect is a geometric effect characterized by the ratio of δ to model radius. Boundary layer calculations were made using 2-foot long elliptical noses, model pressure distributions from Newtonian impact theory, estimated transition locations, and model radii of 3 and 6 inches to estimate the magnitude of this effect. The measured ratios of δr were found to be 0.25 at the second data acquisition station, resulting in an increase in c_f less than or equal to 1.5%, based on the calculations.

5.2.5 Surface Roughness Effects In order to insure that the model was hydraulically smooth, boundary layer calculations were used to determine the $y^+ = 5$ height normal to the surface. Figure 9 shows y in inches plotted against y^+ for the most severe case, that at highest unit Reynolds number. Based on this figure, the rms wall roughness should be smaller than 30 μin. When constructed, the complete model and skin friction balance element had a measured roughness of 4 μ inches and a value of y^+ of about one. Based on the $y^+=5$ criterion, surface roughness should not have significantly affected the skin friction measurements of this test.

5.2.6 Lateral Divergence Effects Three dimensionality of the flow is evident even in flat plate experiments where great care has been taken to insure the two-dimensionality of the outer flow. From velocity profiles measured across the flow, plots of θ are always somewhat ragged, in keeping with skin friction measurements at the same locations and variations in the wake component. This may be due to the raggedness in the transition process, and/or the presence of near-wall structures in the boundary layer, inducing a standing pattern in the flow. When there is finite three dimensionality in the flow, effects are added to the usual two dimensional raggedness. In order to minimize the three dimensionality of the flow on a longitudinal cylinder, the expected droop due to the model weight was calculated and found to be approximately 0.25 degree. Since the model could be adjusted within 0.1 degree, it was felt that the effect could be minimized by careful alignment of the model. Initial runs were devoted to model alignment. In addition, rake, balance, and Preston tube measurements were always made in the same azimuthal plane, which will be

shown to be an important issue in a later section of this report.

5.2.7 Freestream Disturbance Levels The dependence of turbulent c_f and other boundary layer parameters on rms freestream turbulence intensity and length scale has been shown to be nonlinear.[40] For NTF the freestream turbulence level is not known, so this parameter remains a potentially important parameter in the assessment of skin friction measurements made in this tunnel. The main sources of noise in NTF have been identified[41] by measuring surface pressure fluctuations at several places within the tunnel. It is noted that, in comparison with other transonic wind tunnels, the NTF has low levels of test section fluctuating static pressure.

5.3 Profile Measurements — Skin Friction from Clauser Method

5.3.1 Transformed Velocity Profiles The pitot rake was mounted at both Stations 1 and 2. Skin friction coefficients were inferred from velocity profiles by first transforming the data to incompressible form by applying the van Driest transformation and then using the Clauser method of fitting the velocity profile to the law of the wall. Pitot pressures were reduced to Mach numbers assuming isentropic, ideal gas flow, constant gamma, and constant p_s throughout the boundary layer[42]. Since T_t was not measured, the local total temperature in the boundary layer was estimated by the Rotta relation[43]. By this means, both temperature and velocity profiles can be obtained from the Mach number profile along with measurement of T_t and T_w. Despite efforts to locate rake tubes very near the model wall, the first point in the velocity profile was well within the logarithmic layer of the boundary layer, as shown in the velocity profile data of Figure 10 (a) plotted in law-of-the-wall coordinates. In order to accurately calculate boundary layer integral quantities such as δ^* and θ, the theoretical profile of East, also used by Gaudet[16], was used to fill in the profile from the wall to the first data point. The profile of Spalding[7] could also have been used. For the law of the wall k=0.41 and C=5.5 were used. The strength of the wake component was 2.2 for the present data, in agreement with other high Reynolds number data as shown in Reference 44. Transformed profiles are plotted in traditional defect coordinates in Figure 10 (b) and in the coordinates of Reference 4 in Figure 10 (c).

Transformed shape factors are shown in Figure 11 along with the low Reynolds number data of Coles and Purtell, the higher Reynolds number data of Gaudet, and the results from a zero pressure gradient boundary layer calculation. For the calculation of shape factors for data, the value of C used did not affect the values of transformed shape factors significantly.

5.3.2 Inferred Skin Friction Figure 12 shows values of c_f inferred from velocity profiles by the Clauser method plotted as a function of transformed R_θ. The value of skin friction obtained is dependent on the constants used in equation 7. The value of k is usually taken to be 0.41 in the literature and was used for reducing the present data. The value of C chosen by various authors to describe their data usually varies between 5.0 and 5.5. This variation is not surprising since, as pointed out by Coles, the outer part of the boundary layer is extremely sensitive to extraneous effects in the flow. A value of C=5.5 was used for the final reduction of the profile data since this value gave better agreement with Preston tube data, the theory of Spalding, and the results from finite-difference calculations than did 5.0. To decrease the c_f level to that of Karman-Schoenherr, an even higher value of C would have been necessary. Reduction of the data using C=5.0 and 5.5 is shown in Figure 12. A value of 5.0 gave values of c_f too high at Reynolds numbers between 30,000 and 100,000 where other data exists, and for this reason a value of 5.5 was used for the final reduction of the present data.

5.3.2 Circumferential Measurements To check for non-uniform flow effects, rake data were taken at nominal α=0 at ϕ increments of 15 degrees by rolling the model. Data from the pitot rake were reduced to boundary layer parameters, and are shown in Figure 13 (a). Measured skin friction coefficients and values of R_θ show a consistent behavior, *i.e.*, as θ decreases, c_f increases; conversely, as θ increases, c_f decreases.

The c_f data are replotted as a function of R_θ in Figure13 (b). From this figure, it was concluded that when the skin friction is plotted as a function of R_θ, variations in circumferential flow are removed, and also that data from different measuring devices should be taken at the same circumferential location on a model. Two dimensional standing patterns on tunnel walls and models have been found, and the variation is not

always insignificant. For this test, skin friction data was always taken at ϕ=0 and nominal α=0.

There is a significant gradient in the circumferential skin friction coefficient in the vicinity of ϕ=0, where skin friction measurements were made. The Preston tube and rake measurements were essentially point measurements, however the skin friction balance, having an element 3 inches in diameter, subtended an angle of approximately 27 degrees. The skin friction was higher on the counter-clockwise side than at ϕ=0, and lower on the clockwise side.

To provide data for comparison with computational methods, additional runs were made with the model at angle of attack. Data are available from the authors.

5.4 Preston Tube Data

5.4.1 Model Alignment In order to align the model with the incoming flow, Preston tubes were mounted on plugs at six circumferential positions at the two skin friction measurement stations. Preston tube pressures, a measure of the local surface shear, have been shown to be more sensitive to flow angularity than surface pressures[18]. By reducing Preston tube data to skin friction values and plotting the results as a function of angle of attack, the model could be zeroed in relation to the flow, not the test section geometry. No yaw adjustment was possible with the tunnel sting-mounting arrangement; however, the model could be adjusted in angle of attack.

Several runs were devoted initially to aligning the model, with results at Station 2 shown in Figure 14. It was determined that the nominal zero angle of attack was —0.07 degrees, independent of tunnel Mach number. Later runs with the pitot rake installed and the model rolled in 15 degree increments at α= — 0.07deg, confirmed these results by giving essentially the same pressure patterns on rake tubes 1 and 25 as the model was rolled.

5.4.2 Skin Friction Measurements Preston tubes were mounted at Station 2 and data were taken in both ambient temperature air and cold nitrogen flow. The calibration of Patel was used, which was determined from the Princeton Superpipe calibration to be valid at the high Reynolds numbers of this test. Compressibility effects were accounted for by the T method of Sommer and Short[35].

Figure 15 (a) shows the resulting calculated compressible c_f at Mach numbers of 0.4, 0.6, 0.7 and 0.85 as a function of tunnel Re/ft. The spread in c_f at the lowest unit Reynolds number between the Mach 0.4 and Mach 0.85 data is an indication of compressibility effects. In order to plot the data as a function of R_θ, values of θ at each test condition were calculated from the boundary layer survey data. The data in incompressible form are compared with the Karman-Schoenherr and Spalding theories in Figure 15 (b).

5.5 Balance Measurements

The skin friction balance was tested at Station 2 at both hot and cold flow conditions. The resulting data are shown in Figure 16. The data are plotted as compressible c_f against tunnel unit Reynolds number in Figure 16 (a), and also as incompressible c_f against transformed R_θ in Figure 16 (b) for comparison with theory. In incompressible form, the compressible c_f was transformed to incompressible by the T-prime method, and R_θ was taken from velocity profiles at the same location. In most cases the data appear to be significantly higher than incompressible theory, even at Reynolds numbers of 40,000 to 50,000. The reasons for this could not be determined, however, in view of the severe problems encountered in running the balance at cryogenic temperature in the 0.3 Meter TCT, the same problems might be expected in NTF. Also, the balance element footprint was much larger than that of the other devices, making it more susceptible to variations in the circumferential flow.

5.6 Comparison of Three Methods

Data from Preston tubes, velocity profiles, and the skin friction balance are shown in Figure 17. Data from the Preston tubes and velocity profiles are in good agreement. Balance data agrees with the other data at the highest Reynolds numbers, however there is large scatter in the balance data at R_θ of 40,000 to 200,000.

The Preston tube and Clauser-inferred values of c_f agreed well with each other and were fit to a power law, having the following equation:

$$c_f = 0.0097\, R_\theta^{(-0.144)} \qquad (9)$$

The data scatter about this line is within – 2%, as shown in Figure 18. Equation 9 is 1% above the Spalding value and 3% above the Karman-Schoenherr value at R_θ =600,000. It is equal to the Spalding value at R_θ=30,000.

This equation is for incompressible skin friction, being derived from the transformed NTF data in the range 32,680 < R_θ < 619,800. For application to compressible flow, a suitable T-prime equation could be used[35].

6. CONCLUSIONS

Skin friction data at transformed R_θ of 619,800 have been shown to agree with existing incompressible theories within 3% at the highest Reynolds number. At R_θ=30,000, the data are in agreement with the theory of Spalding and slightly above the Karman-Schoenherr correlation. The data obtained by two different methods were in good agreement; however, these data did not agree as well with direct measurements made with a skin friction balance. The scatter in the balance measurements, attributed to mechanical problems with the balance, is a strong factor in deemphasizing this data.

The data is free from pressure gradient effects, but has transverse curvature effects which can increase c_f by as much as 1.5%. Surface roughness should not be an issue. A factor affecting the data may be the freestream turbulence of the NTF tunnel, both in rms turbulence level and in scale. There are indications that the turbulence level is not large, however its effect on the data cannot be quantified.

The data were obtained from nominally incompressible flow at M=0.2 to compressible flow at M=0.85. The van Driest transformation and T-prime method appear to be adequate to remove the compressibility effects.

Acknowledgements The authors wish to thank Dr. Richard Campbell for designing the nose for the NTF model. Also thanks to Dr. Arild Bertelrud for many helpful suggestions concerning the presentation of data and content of this paper.

REFERENCES

1. Smits, A. J. and Marusic, I., "High Reynolds Number Flows: A Challenge for Experiment and Simulation," Paper AIAA-99-3530, 30th AIAA Fluid Dynamics Conference, Norfolk, VA, June 28 - July 1, 1999.

2. Zagarola, M. V., Mean-Flow Scaling of Turbulent Pipe Flow, Ph.D. Thesis, Mechanical and Aerospace Engineering, Princeton University, June 1996.

3. Saric, W. S. and Peterson, J. B., Jr., "Design of High-Reynolds-Number Flat-Plate Experiments in the NTF," Paper AIAA-84-0588, AIAA 13th Aerodynamics Testing Conference, San Deigo, CA, March 5-7, 1984.

4. George, W. K. and Castillo, L., "Zero-pressure-gradient turbulent boundary layer," *Applied Mechanics Reviews*, vol 50, no 12, part 1, December, 1997, pp 689-729.

5. Schoenherr, K. E., "Resistance of Flat Surfaces Moving Through a Fluid," *Transactions SNAME*, 40, 1932, pp 279-313.

6. Landweber, L., "The Frictional Resistance of Flat Plates in Zero Pressure Gradient," Spring Meeting of Society of Naval Architects and Marine Engineers, Boston, MA May 7 & 8, 1953, pp 5-32.

7. Spalding, D. B., "A New Analytical Expression for the Drag of a Flat Plate Valid for Both the Turbulent and Laminar Regimes," *International Journal of Heat and Mass Transfer*, 5, 1962, pp 1133-1138.

8. Spalding, D. B. and Chi, S. W., "The drag of a compressible turbulent boundary layer on a smooth flat plate with and without heat transfer," *Journal of Fluid Mechanics*, vol 18, pt 1, January, 1964, pp 117-143.

9. Ludwieg, H. and Tillmann, W., "Investigations of the Wall-Shearing Stress in Turbulent Boundary Layers," NACA -TM-1285, National Advisory Committee for Aeronautics, May, 1950.

10. Fernholz, H. H. and Finley, P. J., The Incompressible Zero-Pressure-Gradient Turbulent Boundary Layer: An Assessment of the Data, Progress in Aerospace Sciences 32, No. 4, August, 1996, pp 245-311.

11. Coles, D. E. and Hirst, E. A., "Computation of Turbulent Boundary Layers - 1968, AFOSR-IFP-Stanford Conference, Volume II Compiled Data," 1968 AFOSR-IFP-Stanford Conference Stanford University, CA 1968.

12. Fernholz, H. H. and Finley, P. J., "A Critical Compilation of Compressible Turbulent Boundary Layer Data," AGARDograph No. 223, AGARD, 1977.

13. Fernholz, H. H., Finley, P. J. and Mikulla, V., "A Further Compilation of Compressible Boundary Layer Data with a Survey of Turbulence Data.," AGARDograph No. 263, AGARD, November, 1981.

14. Bushnell, D. M., Cary, A. M., Jr. and Holley, B. B., "Mixing Length in Low Reynolds Number Compressible Turbulent Boundary Layers," *AIAA Journal*, 13, No. 8, August, 1975, pp 1119-1121.

15. Dussauge, J.-P., Fernholz, H., Finley, P. J., Smith, R. W., Smits, A. J. and Spina, E. F., "Turbulent Boundary Layers in Subsonic and Supersonic Flow," AGARDpgraph No. 335, July, 1996.
16. Gaudet, L., "Experimental Investigation of the Turbulent Boundary Layer at High Reynolds Numbers and a Mach Number of 0.8," TR 84094, Royal Aircraft Establishment, September, 1984.
17. Winter, K. G. and Gaudet, L., "Turbulent Boundary-Layer Studies at High Reynolds Numbers at Mach Numbers between 0.2 and 2.8," R. & M. No. 3712, Aeronautical Research Council, Ministry of Defence, December, 1970.
18. Motallebi, F., "Mean Flow Study of Two-Dimensional Subsonic Turbulent Boundary Layers," *AIAA Journal*, 32, November, 1994, pp 2153-2161.
19. Fernholz, H. H., Krause, E., Nockemann, M. and Schober, M., "Comparative measurements in the canonical boundary layer at Re,theta < 6 x 10**4 on the wall of the German-Dutch windtunnel (title slightly different from this entry)," *Physics of Fluids*, 7, June, 1995, pp 1275-1281.
20. Coles, D., "The Turbulent Boundary Layer in a Compressible Fluid," R-403-PR, Rand Corp., September, 1962.
21. Purtell, L. P., The Turbulent Boundary Layer at Low Reynolds Number, PhD Thesis, Graduate School, Mechanical Engineering, University of Maryland, 1978.
22. van Driest, E. R., "Turbulent Boundary Layer in Compressible Fluids," *Journal of the Aeronautical Sciences*, 18, no. 3, March, 1951, pp 145-160, 216.
23. Bruce, W. E., Jr., "The U.S. National Transonic Facility, Parts I and II. Papers No. 14 and 15," AGARD-R-722, AGARD, April, 1985.
24. Fuller, D. E., "Guide for Users of the National Transonic Facility," NASA Technical Memorandum 83124, July, 1981.
25. Foster, J. M. and Adcock, J. B., "User's Guide for the National Transonic Facility Research Data System," NASA Technical Memorandum 110242, April 1996.
26. Adcock, J. B., "Real-Gas Effects Associated With One-Dimensional Transonic Flow of Cryogenic Nitrogen," NASA TN D-8274, NASA, December, 76.
27. Harris, J. E. and Blanchard, D. K., "Computer Program for Solving Laminar, Transitional, or Turbulent Compressible Boundary-Layer Equations for Two-Dimensional and Axisymmetric Flow," NASA Technical Memorandum 83207, NASA, Langley, February, 1982.
28. Winter, K. G., "An outline of the techniques available for the measurement of skin friction in turbulent boundary layers," Compressible Turbulent Boundary Layers March 1-5, 1976.
29. Allen, J. M., "Evaluation of Compressible-Flow Preston Tube Calibrations," NASA TN D-7190, May, 1973.
30. Ozarapoglu, V., Measurements in Incompressible Turbulent Flows, Ph.D. Thesis, Laval University, 1973.
31. Allen, J. M., "Reevaluation of Compressible-Flow Preston Tube Calibrations," NASA TM X-3488, February 1977.
32. Patel, V. C., "Calibration of the Preston tube and limitations on its use in pressure gradients," *Journal of Fluid Mechanics*, v 23, pt 1, September, 1965, pp 185-208.
33. Bertelrud, A., "Pipe Flow Calibration of Preston Tubes of Different Diameters and Relative Lengths Including Recommendations on Data Presentation for Best Accuracy," FFA Report 125, Aeronautical Research Institute of Sweden, 1974.
34. Bradshaw, P. and Unsworth, K., "A Note on Preston Tube Calibrations in Compressible Flow," IC Aero Report 73-07, Imperial College of Science and Technology, September, 1973.
35. Sommer, S. C. and Short, B. J., "Free-Flight Measurements of Turbulent-Boundary-Layer Skin Friction in the Presence of Severe Aerodynamic Heating at Mach Numbers from 2.8 to 7.0," NACA-TN-3391, NASA, Ames, March, 1955.
36. Watson, R. D., "Generalized Velocities in the Outer Region of Hypersonic Turbulent Boundary Layers," *AIAA Journal*, 17, Number 8, August, 1979, pp 919-921.
37. Maise, G. and McDonald, H., "Mixing Length and Kinematic Eddy Viscosity in a Compressible boundary Layer," *AIAA Journal*, 6, No. 1, January, 1968, pp 73-80.
38. Clauser, F. H., The Turbulent Boundary Layer, Advances in Applied Mechanics IV, 1956, pp 1-51.
39. White, F. M., Viscous Fluid Flow, McGraw-Hill Book Company, 1974,
40. Hancock, P. E. and Bradshaw, P., "The Effect of Free-Stream Turbulence on Turbulent Boundary Layers," *Journal of Fluids Engineering*, 105, September, 1983, pp 284-289.
41. Igoe, W. B., "Analysis of Fluctuating Static Pressure Measurements in the National Transonic Facility," NASA Technical Paper 3475, NASA, March, 1996.
42. Staff, A. R., "Equations, Tables, and Charts

for Compressible Flow," NACA Report 1135, NASA, 1953.
43. Rotta, J. C., "Critical Review of Experimental Heat Transfer Coefficients and Temperature distributions in Turbulent Boundary Layers at Supersonic and Hypersonic Flow," NASA TTF 10,905, 1967.
44. Gad-el-Hak, M. and Bandyopadhyay, P., "Reynolds number effects in wall-bounded turbulent flows," *Applied Mechanics Reviews*, Vol. 45, No. 8, August, 1994, pp 307-365.

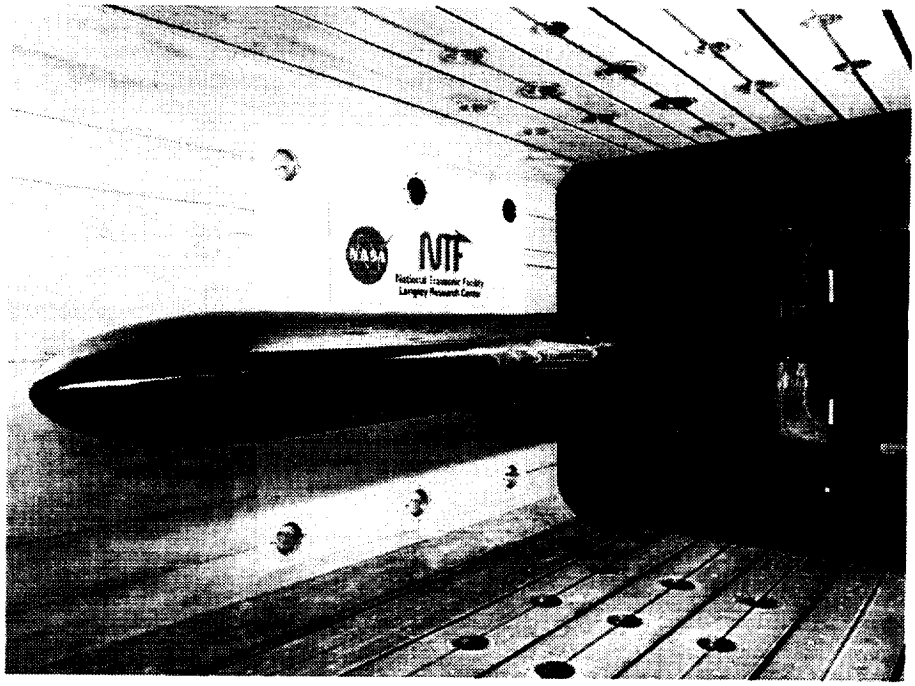

Figure 1. Photograph of Model in NTF.

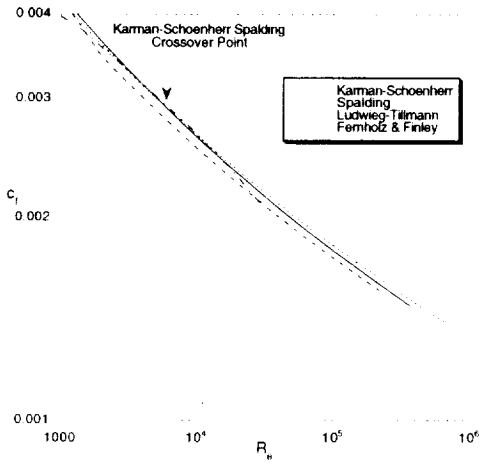

Figure 2. Flat Plate Skin Friction Theories and Correlations.

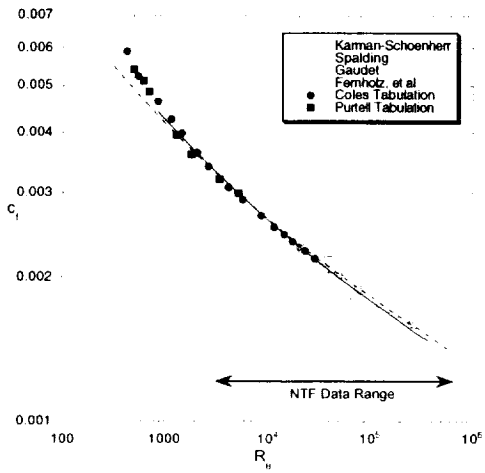

Figure 3. Comparison of Flat Plate Data with Theory.

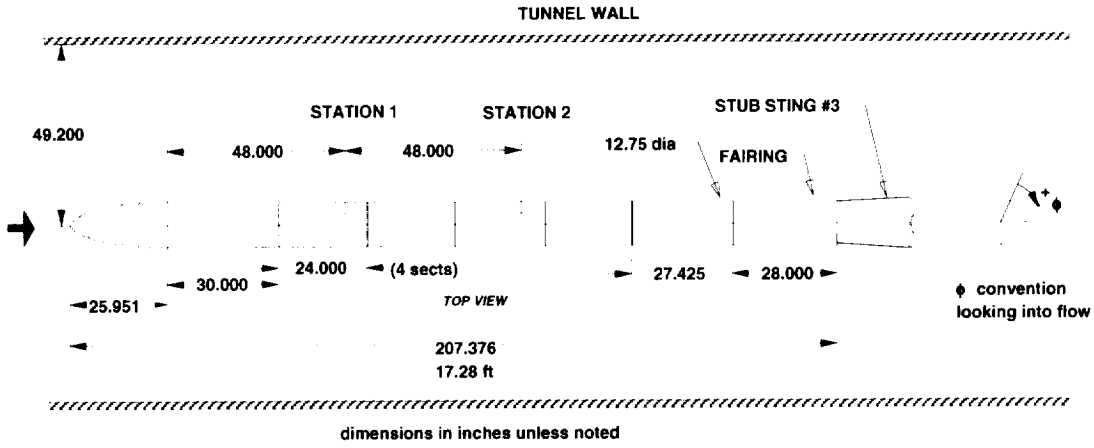

Figure 4. Sketch of Model.

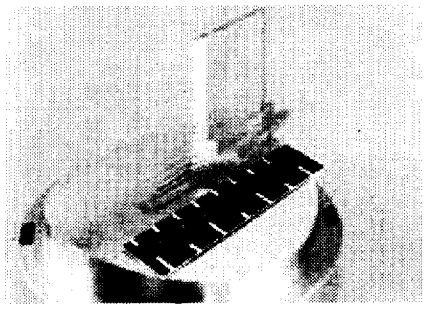

(a) Rake.

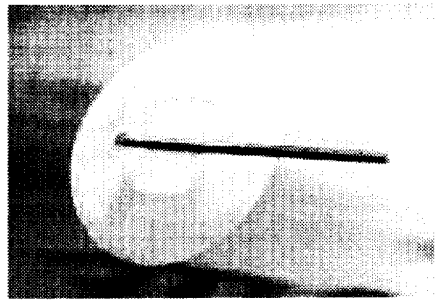

Figure 5. Continued. (b) Preston Tube.

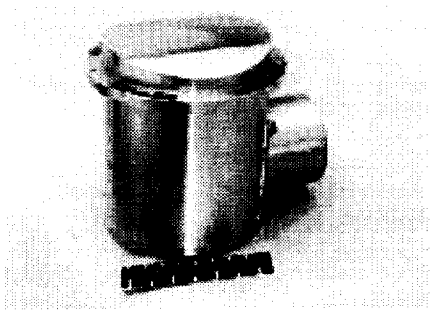

(c) Skin Friction Balance.

Figure 5. NTF Model Instrumentation.

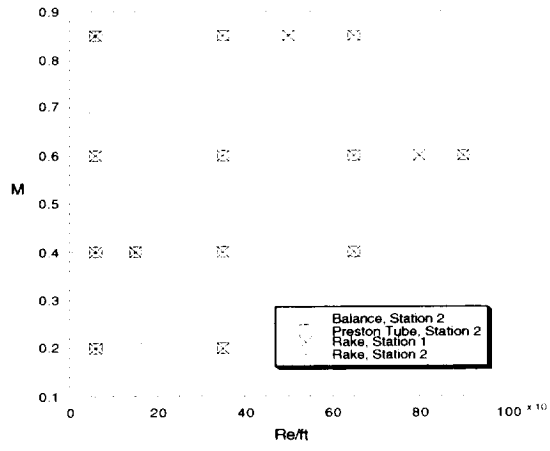

Figure 6. Mach-Reynolds Number Test Conditions.

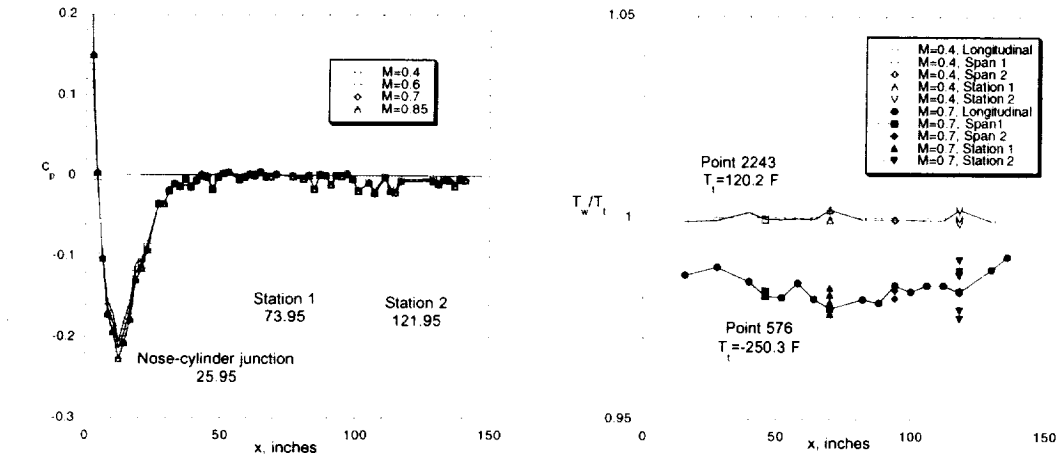

(a) Pressures. (b) Temperatures.

Figure 7. Representative Pressures and Temperatures On Model.

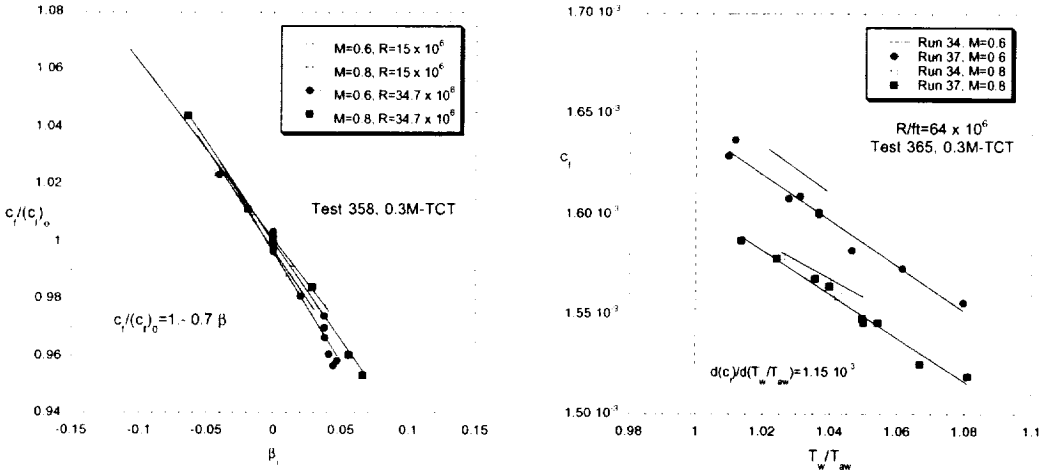

(a) Pressure Gradient Effects. (b) Wall Temperature Effects.

Figure 8. Effects of Pressure Gradient and Wall Temperature on Measured c_f.

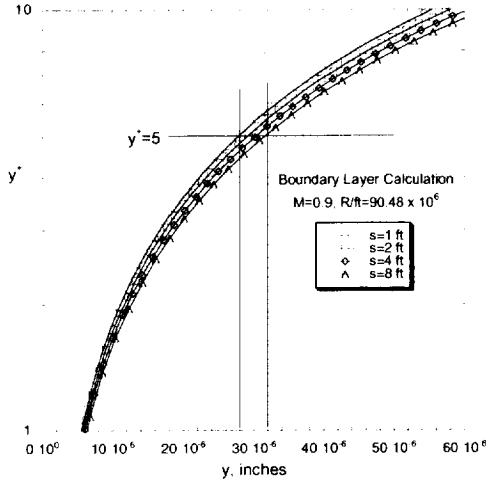

Figure 9. Calculated Turbulent Wall Scaling.

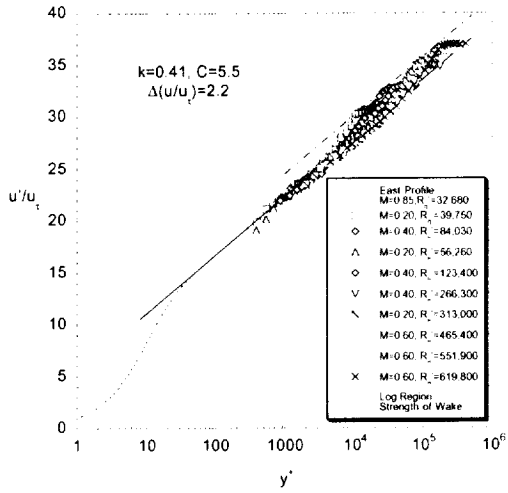

(a) Law-of-Wall.

Figure 10. Transformed Velocity Profiles.

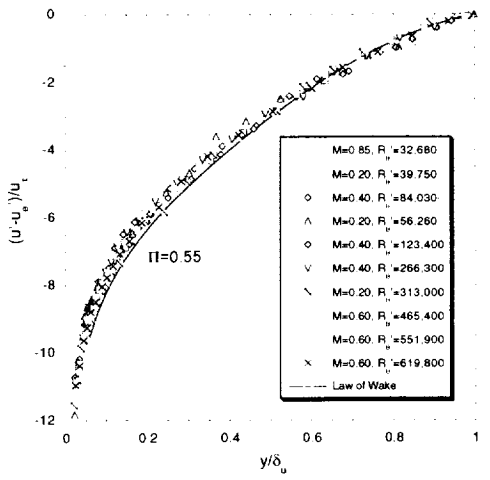

(b) Law-of-Wake.

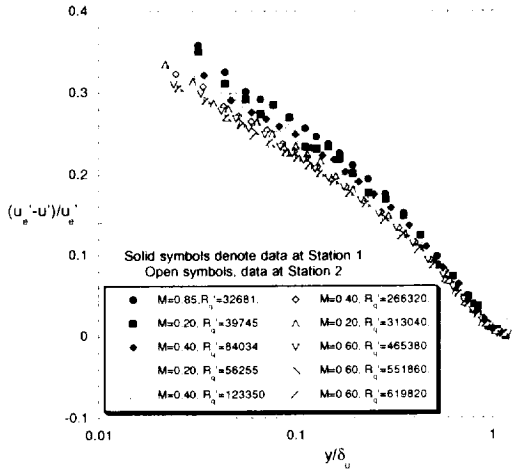

(c) Outer Region

Figure 10. Transformed Velocity Profiles.

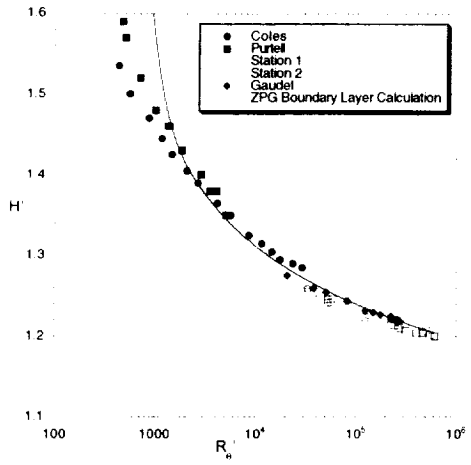

Figure 11. Transformed Shape Factors

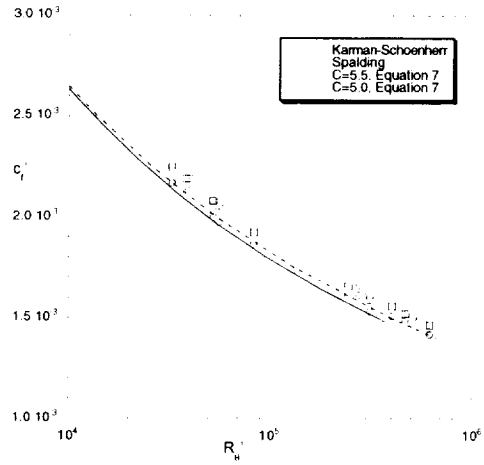

Figure 12. Effect of C on c_f Obtained by Clauser Method.

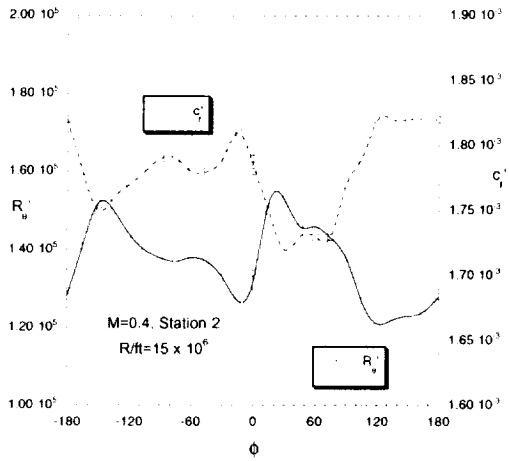

(a) Variation of c_f with ϕ.

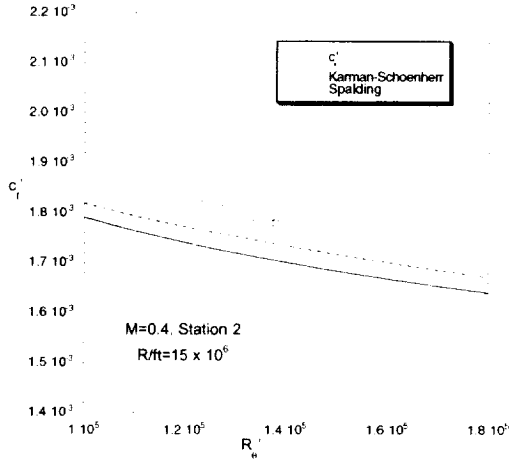

(b) Variation of c_f with R_θ.

Figure 13. Variation of Boundary Layer Properties from Rake with Roll Angle.

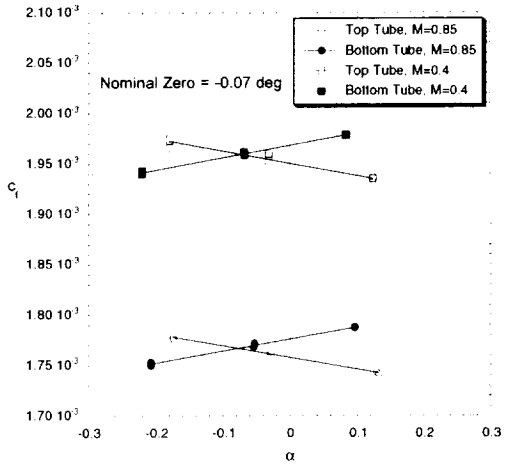

Figure 14. Determination of Nominal Zero Angle of Attack.

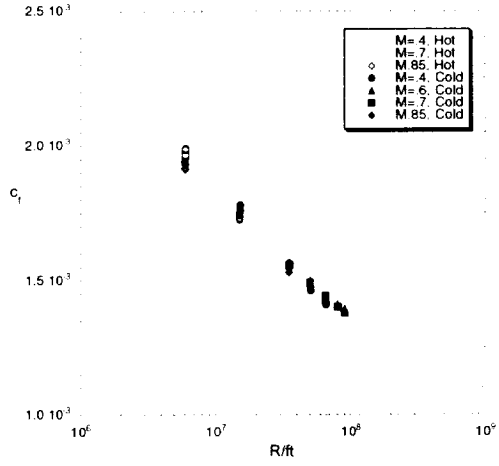

(a)Compressible Data.
Figure 15. Preston Tube Data.

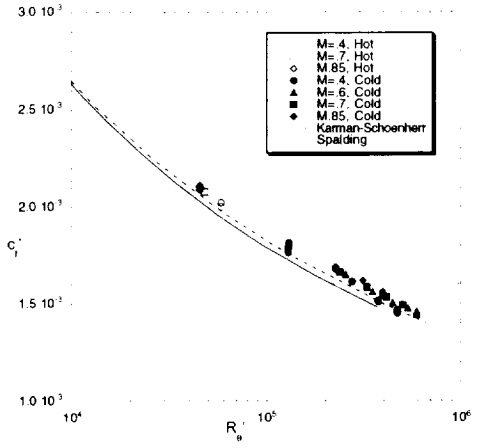

(b) Data in Transformed Parameters.
Figure 15. Concluded.

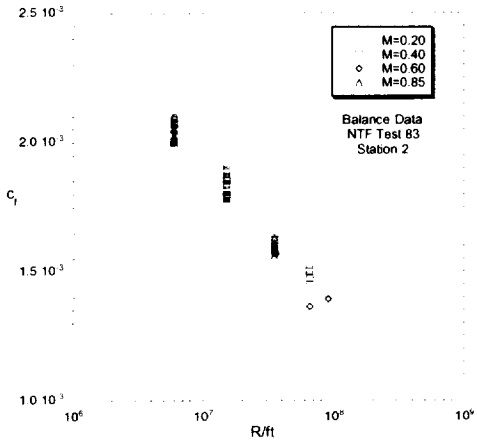

(a) Compressible Data.
Figure 16. Balance Data.

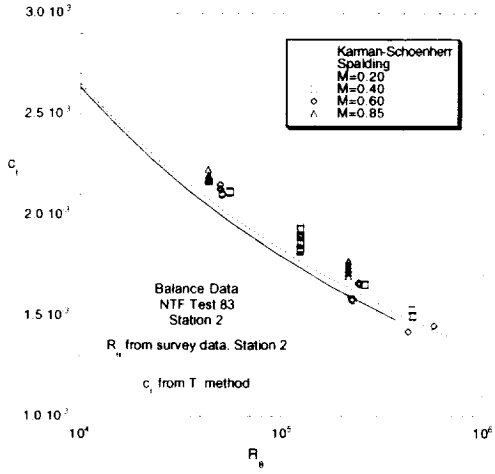

(b) Data in Transformed Parameters.
Figure 16. Concluded.

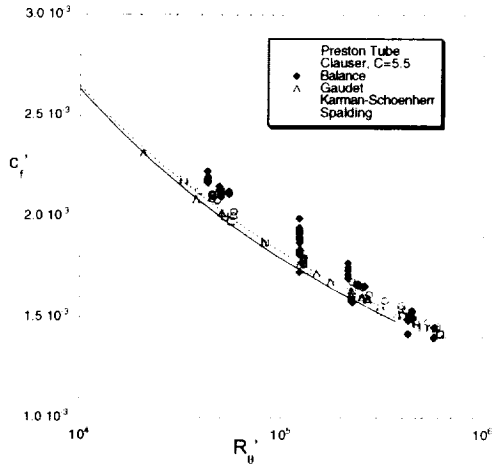

Figure 17 Comparison of Three Measurement Techniques.

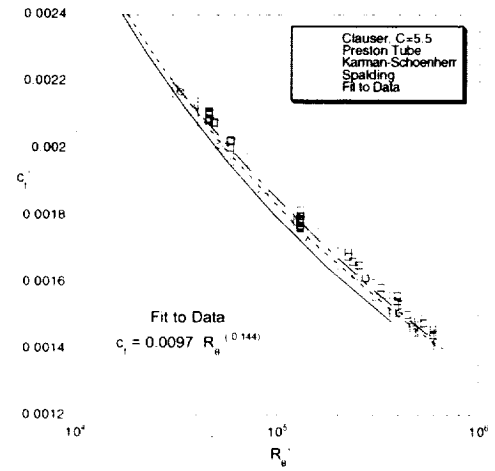

Figure 18. fit to Preston Tube and Crofile c_f Data.